



16 **Abstract**

17 Biogenic volatile organic compounds (BVOCs) exert a significant influence on photochemical air
18 pollution and climate change, with their emissions strongly affected by meteorological conditions.
19 However, the effect of drought on BVOC emissions is not well-characterized, limiting the predictive
20 power of this feedback on climate change and air quality. This study hypothesized that under severe
21 drought conditions, BVOC emissions will be more sensitive to instantaneous intraday variations in
22 meteorological parameters than to the absolute values of those parameters. To test this hypothesis, we
23 employed proton transfer reaction time-of-flight mass spectrometry to quantify the mixing ratios of a
24 suite of soluble and insoluble VOCs, including isoprene, monoterpenes, sesquiterpenes, acetone,
25 acetaldehyde, methanol, ethanol, formaldehyde, formic acid, acetic acid, 1,3-butadiene, dimethyl
26 sulfide (DMS), and H₂S, under severe drought conditions in a natural Eastern Mediterranean forest in
27 autumn 2016. Except for H₂S, which was used as a control, and to a certain extent DMS, all measured
28 VOCs exhibited a strong response to changes in relative humidity, with lower mixing ratios observed
29 around noon, suggesting inhibition of BVOC emission under the relatively high temperature and low
30 relative humidity of drought conditions. Notably, our analysis revealed that instantaneous changes in
31 meteorological conditions, especially in relative humidity, can serve as a better proxy for drought-
32 related changes in BVOC emission rate than the absolute values of meteorological parameters. These
33 findings are supported by direct flux measurements conducted in a mixed Mediterranean forest under
34 drought conditions, in the same region, and presented as a companion article. The findings further
35 highlight the importance of analyzing the effect of meteorological conditions on BVOC emissions
36 under drought conditions on a daily—or shorter—timescale, and support biogenic emission sources
37 for 1,3-butadiene.



38 **1 Introduction**

39 Biogenic volatile organic compounds (BVOCs) are an important factor for accurate modeling of
40 climate change and photochemical air pollution (Calfapietra et al., 2013; Curci et al., 2009; Peñuelas
41 et al., 2009; Harper and Unger, 2018). BVOCs are thought to be emitted to protect the vegetation from
42 biotic and abiotic stresses (Peñuelas and Munné-Bosch, 2005; Blande et al., 2007; Brillì et al., 2009;
43 Berg et al., 2013), and for plant–plant and plant–animal communication (Baldwin et al., 2006; Filella
44 et al., 2013; Trowbridge and Stoy, 2013). The emission rate of BVOCs depends on their rate of
45 synthesis, physicochemical properties, and ambient conditions (Niinemets and Monson, 2013).
46 Climate change leads to a significant change in the emission rate and composition of BVOCs. For
47 instance, the emission rate of most BVOCs increases with temperature in an Arrhenius-type manner
48 (Goldstein et al., 2004; Guenther et al., 1995; Monson et al., 1992; Niinemets et al., 2004; Tingey et
49 al., 1990). However, drought can affect the emission and composition of BVOCs in a more complex
50 manner (Fortunati et al., 2008; Peñuelas and Staudt, 2010; Holopainen and Gershenson, 2010; Llusia
51 et al., 2016; Schade et al., 1999), which is currently not well-characterized. Enhancing our
52 understanding of the intricate mechanisms through which climate change influences BVOC emissions
53 is crucial for improving model simulations and assessments of air quality and climate.

54 Drought affects the emission of BVOCs primarily via stomatal resistance, which is typically 2
55 orders of magnitude larger than cuticular resistance (Nobel, 1999). Hence, the effect of drought on
56 BVOC emissions depends on environmental conditions, such as the level of the drought, and it is
57 further complicated by plant types and properties, as well as the specific BVOC species. Soluble
58 BVOCs such as alcohols and carboxylic acids, with Henry’s law constants (H) on the order of 10^{-2} –
59 $10^1 \text{ Pa m}^3 \text{ mol}^{-1}$, are generally more sensitive to stomatal conductance than non-soluble BVOCs
60 (Niinemets et al., 2004; Niinemets and Reichstein, 2003; Harley, 2013). However, these soluble



61 species may be emitted at high rates under higher relative humidity (RH) during periods of drought
62 (Filella et al., 2009; Loreto and Schnitzler, 2010).

63 The effect of drought on isoprene emission has been studied extensively and was shown to be
64 delayed and/or smaller compared to its effect on photosynthesis rate (Tiiva et al., 2009; Niinemets,
65 2010; Zheng et al., 2017). Under moderate drought stress, only a moderate decrease or increase of
66 isoprene was reported, but isoprene emission tends to decrease more significantly under more severe
67 or prolonged drought stress (Pegoraro et al., 2005; Pegoraro et al., 2004; Sharkey and Loreto, 1993;
68 Potosnak et al., 2014; Brillì et al., 2007). The effect of drought on the emission of other BVOCs, such
69 as monoterpenes (MTs) and sesquiterpenes (SQTs), has been less extensively studied, but there is
70 accumulating evidence of different responses to drought compared to isoprene, particularly for SQTs.
71 SQT emission was shown to be less significantly reduced by moderate drought stress than that of MTs,
72 isoprene, and some oxygenated BVOCs, with a potential rise close to the wilting point (Ormeño et al.,
73 2007; Kreuzwieser et al., 2021; Hansen and Seufert, 1999; Bonn et al., 2019). According to Moradi et
74 al. (2017), the effect of drought stress on terpenes such as MTs and SQTs also depends on the
75 sensitivity of the specific plants to drought stress, where in more tolerant plants, either increased or
76 stable emission rates of SQTs and MTs can occur under relatively prolonged stress.

77 The way in which meteorological conditions affect BVOC emission under drought conditions
78 should be strongly related to their effect on stomatal conductance (Niinemets and Monson, 2013;
79 Nobel, 2009). Under these conditions, stomatal conductance typically demonstrates morning and
80 afternoon peaks, associated with the so-called midday depression (e.g., Li et al., 2019; Seco et al.,
81 2017). Notably, these peaks are typically accompanied by a monotonic trend in RH and temperature.
82 Hence, we hypothesize that stomatal conductance and consequently, BVOC emissions, are more
83 sensitive to intraday variations in meteorological conditions than to the absolute values of those



84 parameters. This hypothesis is also supported by the fact that the morning peaks in BVOC emissions
85 often coincide with temperature and RH values that differ significantly from those associated with the
86 afternoon peaks.

87 Previous studies in the Eastern Mediterranean have indicated that activity of the natural
88 vegetation in this region tends to decrease under prolonged drought conditions in the absence of rain
89 events (Maseyk et al., 2008; Rohatyn et al., 2018). Furthermore, Llusia et al. (2016) showed that during
90 spring and summer in the Eastern Mediterranean, terpene emission rates are enhanced by warmer
91 summer conditions but are strongly reduced under severe drought conditions. The Eastern
92 Mediterranean is recognized as a global warming hotspot (Giorgi, 2006; IPCC, 2007; Lelieveld et al.,
93 2012), associated with increasing drought conditions (Cook et al., 2016; Hoerling et al., 2012),
94 particularly during the autumn (Li et al., 2019). Hence, we assumed that field measurements in this
95 region during the autumn, under severe drought conditions, could be used to test our hypothesis and
96 provide important insights into the effect of meteorological parameters on BVOC emission under
97 drought.

98

99 **2 Methods**

100 ***2.1 Experimental site***

101 The field measurements were carried out at the Beit Keshet Forest (Shibli) site (32.704680 N,
102 35.386608 E), located 36 km from the Eastern Mediterranean coast of northern Israel (see Fig. 1), at
103 an elevation of 202 m above mean sea level. The site is approximately 1200 m × 900 m of moderate
104 homogeneous slope, within a ca. 1000 ha forest covered by ~25% *Quercus calliprinos*, ~25% *Quercus*
105 *ithaburensis*, ~20% *Pistacia terebinthus*, ~15% *Pistacia lentiscus*, ~10% *Pinus halepensis*, and ~5%
106 *Pinus pinea*. Average canopy height is approximately 5 m. The site is exposed to a Mediterranean



107 climate with an annual precipitation of 486 mm, and mean daily maximum and minimum temperatures
108 of 27.4 °C and 15.0 °C, respectively.

109

110 *2.2 Field measurements*

111 The measurements at the Shibli site were performed between 6 Sep and 7 Nov 2016, and are described
112 in more detail in (Li et al., 2019). The instrumentation setup included a platform for eddy covariance
113 (EC) measurements of VOCs, ozone (O₃), carbon dioxide (CO₂) and water vapor (H₂O), sensible heat,
114 latent heat, and momentum, as well as slower O₃ and NO_x measurements in an air-conditioned mobile
115 laboratory which was located about 5 m from the EC tower, and another tower that was used for
116 measurements of basic meteorological parameters. Note that due to a technical problem—a lack of
117 synchronization resulting from the proton transfer reaction time-of-flight mass spectrometry (PTR-
118 ToF-MS) data not being consistently recorded at the specified frequency of 10 Hz, VOC fluxes were
119 not evaluated.

120 The VOC measurements were performed using a PTR-ToF-MS 8000 (Ionicon Analytik GmbH,
121 Innsbruck, Austria; see (Graus et al., 2010; Jordan et al., 2009), as described in more detail in Dayan
122 et al. (2020). Ambient air was pulled at a rate of about 35 L min⁻¹ through a PFA Teflon tube (3/8 inch
123 outer diameter, 5/16 inch inner diameter) and was directed to PTR-ToF-MS for sampling at a rate of
124 0.5 L min⁻¹ through a 1/16 inch outer diameter polyether ether ketone tube. The measured data were
125 recorded in a computer at a frequency of 10 Hz. The background (zero) and sensitivity (span)
126 calibrations were performed every 3 h and weekly, respectively. Zero air for background calibration
127 was obtained through a catalytic converter which was heated to 350 °C. Gas standards (Ionicon
128 Analytik GmbH) were used for the sensitivity calibration. The raw hdf5 data files of the PTR-ToF-MS
129 were preprocessed using PTRwid processing suite in the IDL environment (Holzinger, 2015). The EC



130 measurements were performed at 10 Hz using a 3D anemometer (R3-100, Gill Instruments, Hampshire,
131 UK). A fast closed-path dry chemiluminescent O₃ sensor (FOS V2.0.1, Sextant, New Zealand) and an
132 open-path CO₂/H₂O gas analyzer (IRGA; LI-7500, LI-COR, Lincoln, NE, USA) were used to quantify
133 the fluxes of O₃ and CO₂/H₂O, respectively.

134 O₃ mixing ratios were measured using a model 49i (Thermo Environmental Instruments
135 Inc., Waltham, MA, USA) with a limit of detection of 1.0. Complementary meteorological
136 measurements included wind speed and direction using an R.M. Young wind monitor 05103,
137 temperature (T) and RH using a Campbell HC2S3 probe, and net radiation using a Kipp & Zonen
138 CMP11 probe. The FOS, IRGA and sonic 3D data were recorded to a CR3000 data logger (Campbell
139 Scientific, Logan, UT, USA) at a frequency of 10 Hz. T, RH, net radiation, O₃, and NO_x mixing ratio
140 were recorded by a CR1000 data logger (Campbell Scientific) at 1 min time resolution.

141

142 ***2.3 Flux evaluation and partitioning***

143 Flux evaluation and partitioning are described in more detail in (Li et al., 2019). Briefly, the fluxes of
144 CO₂, H₂O, and O₃ were evaluated using the EddyPro 6.2.0 software (LI-COR), and partitioning of the
145 fluxes to stomatal and non-stomatal flux was performed using the electric circuit analogy (Chamberlain
146 and Chadwick, 1953). Daytime carbon assimilation (A) was evaluated by subtracting the respiration
147 flux from the net measured CO₂ flux, individually for each diurnal cycle. The daytime respiration flux
148 was evaluated by extrapolating the nighttime measured CO₂ flux, which presumably represents solely
149 the respiration flux, according to Reichstein et al. (2005).

150



151 *2.4 Modeling of BVOC emission rate*

152 BVOC emission rates were evaluated using the Model of Emissions of Gases and Aerosols from
153 Nature version 2.1 (MEGANv2.1; (Guenther et al., 2012), with an updated algorithm for the
154 parameterized drought stress (Wang et al., 2022)). The major driving variables input into the model
155 were species composition, light, leaf area index, vegetation cover fraction, T, and soil moisture. The
156 model was configured using actual meteorological data measured onsite. Vegetation cover fraction
157 and leaf area index inputs were determined using remote sensing (MOD44B and TERRA/MODIS,
158 respectively). Root fraction was estimated based on soil samples collected in the region of the
159 measurements. The wilting point was estimated based on the soil type as discussed for the specific
160 measurement region in Ravikovitch et al. (1960).



161

162 **Figure 1.** Regional satellite image including the Shibli site. Background imagery from © Microsoft Bing Maps.



163 **3 Results and discussion**

164 ***3.1 Identified VOCs used for the analyses***

165 The following analyses rely on the assumption that the BVOC mixing ratios which were measured
166 over the studied vegetation can be used as a proxy for their emission rate from the vegetation, and that
167 this, in turn, will enable us to study the effect of meteorological conditions on the BVOC emission rate.
168 However, considering that the correlation between meteorological conditions and mixing ratios can be
169 indirectly affected by the impact of meteorological conditions on the mixing height and chemical loss
170 rate, we also focus on VOCs that presumably originated predominantly from anthropogenic sources as
171 a control.

172 Anthropogenic VOCs (AVOCs) presumably include 1,3-butadiene ($m/z = 55.055$) (Knighton
173 et al., 2009) and hydrogen sulfide (H_2S) ($m/z = 34.995$) (Li et al., 2014); however, our analyses
174 indicated that the former is predominantly emitted from biogenic sources during the measurements.
175 BVOCs presumably include MTs ($m/z = 137.133$, $m/z = 95.086$, $m/z = 81.070$), isoprene + 2-methyl-
176 3-buten-2-ol (MBO) ($m/z = 69.071$; $m/z = 69$), dimethyl sulfide (DMS) ($m/z = 63.062$), acetone ($m/z =$
177 59.049), acetaldehyde ($m/z = 45.033$), the sum of methyl vinyl ketone and methacrolein
178 (MVK + MACR) ($m/z = 71.048$) (Janson and Serves, 2001; Karl et al., 2003; Park et al., 2013; Kanda
179 and Tsuruta, 1995), ethanol ($m/z = 47.0497$), methanol ($m/z = 33.032$), formic acid ($m/z = 47.0133$),
180 acetic acid ($m/z = 61.029$), and SQTs ($m/z = 205.195$) (Jordan et al., 2009; Park et al., 2013). This
181 classification is based on the correlation of the VOCs with meteorological parameters, as described in
182 Sect. 3.3 and 3.4, as well as on our previous analysis of measurements in a mixed Mediterranean
183 vegetation site in Ramat Hanadiv (located 44.4 km southwest of the Shibli site (Dayan et al., 2020)).
184 Table 1 compares the observed BVOC mixing ratios with the predicted emission rates for the different
185 BVOCs based on the MEGAN simulations. The mixing ratios are presented for day of year (DOY)



186 306 and 309–313, for which high-quality measurements are available. It is remarkable to note that the
 187 SQT levels are higher than those of the MTs by about 1.5 orders of magnitude, emphasizing the
 188 relevance of the measurement site in studying the effects of drought on atmospheric chemistry via
 189 changes in SQT emission.

190

191 **Table 1.** Comparison of mean and standard deviation of BVOC emission rates as predicted by MEGAN and the observed
 192 mixing ratios, for day of year (DOY) 306 and 309–313. The values are scaled on a white–red color scale, individually for
 193 each column in the table.

194

195

196

197

198

199

200

201

202

203

Compounds	MEGAN (mg m ⁻² h ⁻¹)		Measurement (ppbv)	
	Mean	Standard deviation	Mean	Standard deviation
Isoprene+MBO	3.887E-03	1.656E-02	0.081	0.029
Total MTs	11.142	10.815	0.144	0.078
Myrcene	0.534	0.518		
Sabinene	1.112	1.079		
Limonene	1.631	1.583		
3-Carene	0.541	0.525		
t-β-Ocimene	1.631	1.583		
β-Pinene	1.705	1.655		
α-Pinene	3.262	3.166		
Other MTs	0.726	0.705		
Total SQTs	1.217	1.967	2.718	0.694
α-Farnescene	0.152	0.246		
β-Caryophyllene	0.304	0.492		
Other SQTs	0.761	1.229		
Total MT+SQT	12.359	12.782	2.863	0.772
Methanol	4.802	8.171	2.740	1.333
Acetone	2.406	1.579	2.875	0.652
Bidirectional VOCs	1.786	4.069		
Stress VOCs	1.348	2.587		
Other VOCs	1.403	0.921		
DMS	0.000	0.000	0.078	0.029
Acetaldehyde	0.000	0.000	1.521	0.426



204 *3.2 Spatial heterogeneity in the measured VOCs' mixing ratios*

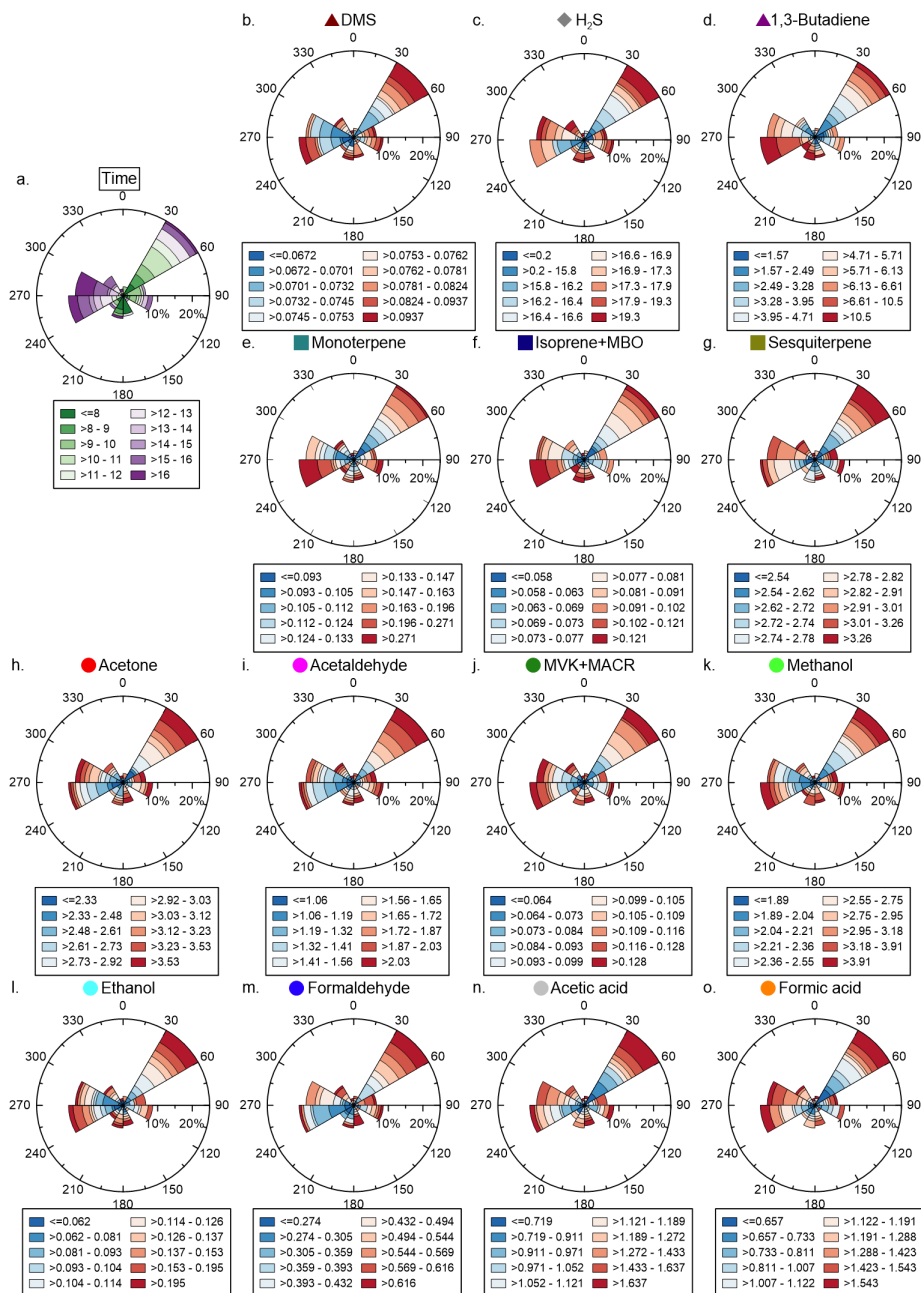
205 Spatial non-homogeneity in the measured VOCs' mixing ratios for different wind directions can affect
206 the interpretation of the effect of changing meteorological conditions on the measured mixing ratios.
207 Such non-homogeneity may result from heterogeneous spatial transport of the measured VOCs from
208 outside the investigated measurement area, or to non-homogeneity in the emission of the BVOCs
209 within the study area due to spatial variations in the vegetation cover and type and/or soil properties.

210 Figure 2 presents, individually for each of the investigated VOCs, the percentage of time that
211 the daytime-investigated VOCs' mixing ratios (Fig. 2b-o) and time (Fig. 2a) fall in a specific range for
212 12 equally sized wind direction ranges. Figure 2a clearly demonstrates the role of sea and land breezes
213 in determining the wind direction during the day: in the morning, air masses mostly originated from
214 the eastern and southern sectors, while in the afternoon, they originated mostly from the western sector.
215 This may lead to difficulty in interpreting the reason for changes in the measured BVOC mixing ratios
216 for different wind directions, considering that both wind direction and meteorological conditions, such
217 as solar radiation, T, and RH, change with time in a systematic manner during the day. Sea and land
218 breezes can also cause systematic differences in the air moisture in the measurement area, for different
219 wind directions and time, directly affecting the BVOCs' emission rates and mixing ratios. Note that
220 the sea breeze has been shown to transport moisture from the Eastern Mediterranean Sea to over tens
221 of kilometers from the coast (Li et al., 2019; Derimian et al., 2017; Naor et al., 2017).

222 Overall, Fig. 2 demonstrates a weak association between the measured VOCs and wind
223 direction. DMS, H₂S, MVK + MACR, and formic acid showed no clear association with wind direction
224 during the daytime. For 1,3-butadiene, isoprene + MBO, and MT, elevated daytime mixing ratios
225 originated predominantly from the southwestern sector. SQT, acetone, acetaldehyde, ethanol,
226 formaldehyde, and acetic acid were associated with somewhat elevated mixing ratios for the



227 northeastern sector during the daytime. In Sect. 3.3 and 3.4, the association of the measured VOCs
 228 with meteorological parameters is investigated.



229



230 **Figure 2.** Mixing ratio vs. wind direction for selected VOCs during the daytime. Presented is the percentage of time for
231 which the measured mixing ratios of VOCs fall in a specific range, specified by an evenly distributed color scale,
232 individually for each of 12 wind sectors. Circular symbols represent presumed soluble BVOCs, square symbols represent
233 presumed insoluble BVOCs, rhombus symbols represent presumed AVOCs, and triangular symbols represent either
234 presumed AVOCs or insoluble BVOCs. See more information on VOC solubility in Table 2.

235

236

237 *3.3 Drought effect on vegetation activity and measured VOC mixing ratios*

238 The Eastern Mediterranean region experiences a notable scarcity of rainfall during the summer, leading
239 to drought conditions at the end of the summer and beginning of autumn. For instance, the mean
240 integrated precipitation amounts between May/June and September/October for the years 2013–2023,
241 recorded at the Tavor Kadoorie station located 2 km from the measurement site near Shibli, is only
242 14.1 mm. It is remarkable that in 2016, daily precipitation was consistently below 1.1 mm for 157 days
243 until DOY 306, the first day included in our analysis. The drought that develops at the end of summer
244 and in early autumn affects BVOC emissions in the Eastern Mediterranean (Li et al., 2019; Llusia et
245 al., 2016; Rohatyn et al., 2018). To verify drought conditions during the field measurements, we used
246 calculated stomatal CO₂ flux as a proxy for vegetation activity in the footprint area. Figure 3 presents
247 the ecosystem gross primary production (GPP) CO₂ flux, net measured water flux, and RH for DOY
248 283–313 (9 Oct–8 Nov; Fig. 3a), and for DOY 306 – 313 (1 Nov–8 Nov), the measured ecosystem
249 GPP CO₂ flux and net water vapor flux (Fig. 3b), and measured T, RH, and vapor pressure deficit
250 (VPD) (Fig. 3c). The analyses presented herein focus on DOY 306 and DOY 309–313, for which high-
251 quality VOC measurements are available. Both DOY 283–313 and DOY 306–313 were characterized
252 by apparently low vegetation activity with a mean daytime stomatal CO₂ flux of 4.16 and 0.70 μmol
253 s⁻¹ m⁻², respectively. As indicated in Fig. 3c, DOY 306–313 was characterized by low RH, down to



254 less than 30%, with a daily minimum at 12:30 h. These low RH levels corresponded with relatively
255 high T and VPD values.

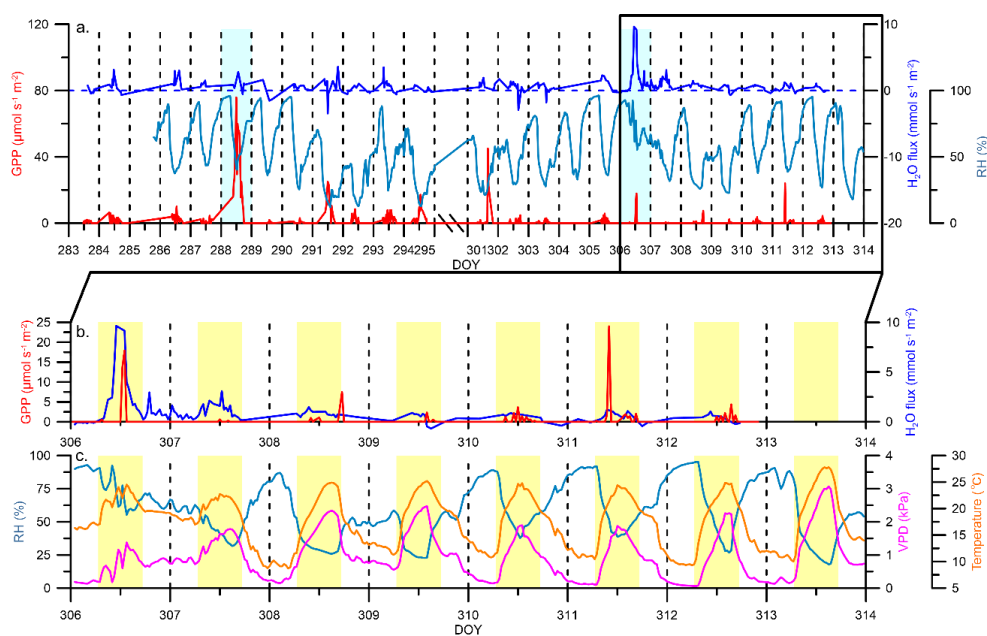
256 Low vegetation activity during the summer and autumn is typical for the Eastern Mediterranean
257 and particularly for the measurement area (Li et al., 2019). For instance, the calculated mean diurnal
258 net CO₂ flux during the autumn in Ramat Hanadiv (located 44.4 km southwest of the site) was 1.0
259 $\mu\text{mol s}^{-1} \text{m}^{-2}$ in 2015–2016, compared to 0.2 and $-2.6 \mu\text{mol s}^{-1} \text{m}^{-2}$ in the winter and spring, respectively.
260 The corresponding mean seasonal net ecosystem production (NEP) for the measurement period is 21.6
261 g C m^{-2} , significantly lower than the mean seasonal NEP in Ramat Hanadiv during the spring (241 g
262 C m^{-2} ; see Fig. S1).

263 DOY 306 was an exception. On this day, a rain event was recorded, resulting in relatively high
264 stomatal CO₂ and evapotranspiration fluxes between 10:00 and 12:00 h, while GPP dropped back from
265 15.84 to 0.01 $\mu\text{mol s}^{-1} \text{m}^{-2}$ at 13:00 h (Fig. 3b). The relatively high evapotranspiration flux on that day
266 was followed by a positive CO₂ flux, which can be explained by the enhanced respiration (see Fig. S2).
267 Relatively high stomatal CO₂ flux also occurred on DOY 311, which can be attributed to the relatively
268 high RH on this specific day (Figs. 3b, 3c).

269 No clear diurnal pattern was observed for the stomatal CO₂ flux, which was nearly zero during
270 all or most of the day, between DOY 306 and DOY 311. Therefore, it was not possible to use CO₂ flux
271 as a proxy for vegetation activity during the day. Instead, we used the meteorological parameters as
272 potential proxies for the regulation of BVOC emission under drought stress, via their effect on stomatal
273 conductance (Sect. 1). Based on the data presented in Fig. 3c, minimum daily RH was lower than 35%
274 for all days except DOY 306, with a minimum daily RH of 55%, and reached as low as 18% on DOY
275 313. While day-to-day changes in T were relatively more moderate than those in RH, day-to-day
276 changes in VPD were also relatively large (Fig. 3c). We hypothesized that these day-to-day and



277 intraday changes in RH and VPD can be used as good proxies for the observed changes in BVOC
 278 mixing ratios under drought conditions. In the following, we investigate the response of the measured
 279 VOC mixing ratios to changes in RH, T, VPD, and global solar radiation (GSR) as proxies for the
 280 effect of meteorological conditions on BVOC emissions under drought stress.



281

282 **Figure 3.** Drought and rain effects on vegetation activity. (a) Measured H₂O flux (blue), ecosystem gross primary
 283 production (GPP) CO₂ flux (red), and RH (cyan) on DOY 283–313. Shaded blue rectangle represents rain event. (b)
 284 Measured ecosystem GPP CO₂ flux and net H₂O flux on DOY 306–313. (c) Measured T, VPD, and RH on DOY 306–313.
 285 Yellow shading represents daytime.

286

287

288 Figure 4 presents the mean measured daytime time series of the various investigated VOCs,
 289 together with the corresponding T, RH, and GSR. In general, the VOCs showed an increase in mixing
 290 ratios following sunrise at ~06:00 h until around 08:00–10:00 h, along with the increasing T, as can be
 291 expected for BVOCs, including soluble BVOCs under drought, during periods of relatively high RH
 (e.g., Filella et al., 2009; Loreto and Schnitzler, 2010). This increase was followed by either a sharp



292 decrease or moderation in the mixing ratios of most presumed BVOCs. For most of the presumed
293 BVOCs, an increase in mixing ratios was observed after around 13:00 h. This contradicts the
294 expectation of an increase in BVOCs during the daytime with temperature (Niinemets and Monson,
295 2013), suggesting a reduction in stomatal conductance and reduced BVOC emissions under severe
296 drought conditions around noontime (Bourtsoukidis et al., 2014; Loewenstein and Pallardy, 1998).
297 SQT and ethanol were exceptional, with no increase in the mixing ratios after 13:00 h for the former,
298 and a late increase in the mixing ratios, starting at around 15:00 h, for the latter. Formic acid was also
299 exceptional in showing a gradual increase in the mean mixing ratios from sunrise to around 12:30 h.
300 Overall, Fig. 4 indicates a drought stress-induced anomaly in the BVOC mixing ratios, which were
301 expected to correlate with GSR and T, resulting in a daytime increase from morning to afternoon.

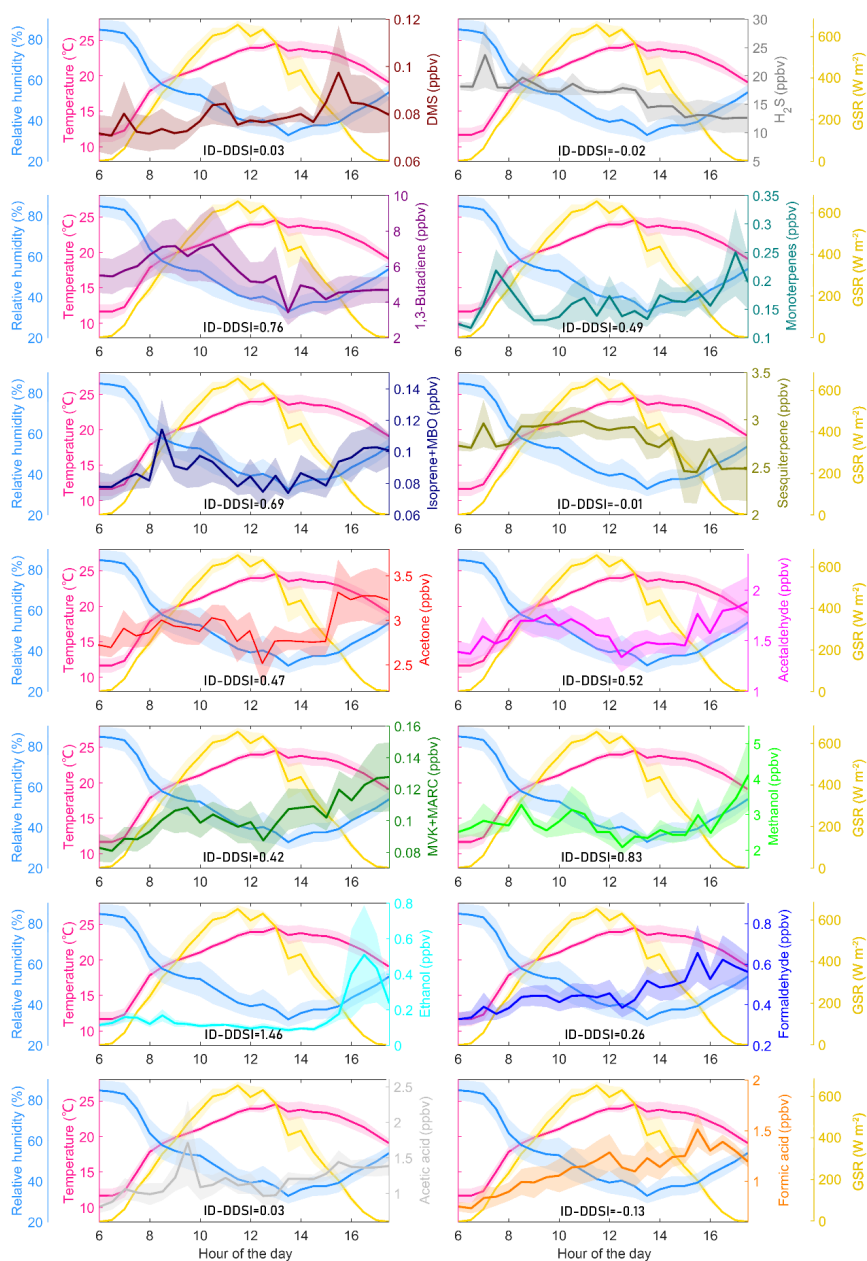
302 To systematically characterize the midday depression in VOC mixing ratios, we calculated
303 both the morning decreasing rate of VOCs between 08:30 and 12:30 h and their afternoon increasing
304 rate from 12:30 h to sunset (17:30 h). We chose 08:30 h to initiate the calculation because most of the
305 BVOC species showed an increase in concentration before this time point, as would be expected for
306 increases in T and GSR under non-drought stress conditions (see Sect. 1). We chose 12:30 h as the
307 turning time point because at this time, the sum over the normalized mixing ratios of each individual
308 presumed BVOC was lowest between sunrise and sunset, corresponding with the lowest mean daytime
309 RH. Accordingly, the intensity of the daytime drought stress index (DDSI) in the VOC mixing ratios
310 was evaluated according to the following equation:

$$311 \quad \text{DDSI} = - \sum_{t=8.5,0.5}^{12.5} \frac{C_{t+0.5} - C_t}{C_t} + \sum_{t=13.0,0.5}^{17.5} \frac{C_{t+0.5} - C_t}{C_t} \quad \text{Eq.1}$$

312 where DDSI represents the intensity of the midday depression and C_t is the mixing ratio at time point
313 t . We repeated the DDSI calculation using a second-order polynomial fitting (DDSI-PF) approach.
314 According to this calculation, DDSI-PF is the difference between the value of this polynomial fitting



315 at 12:30 h and the corresponding value at 12:30 h of a linear line between 08:30 h and sunset (i.e.,
 316 17:30 h). Whereas the former DDSI method (termed in the following as integrated differential [ID]



341 **Figure 4.** Daytime diurnal profiles of the measured VOC species and several meteorological factors (temperature, T;
 342 relative humidity, RH; and global solar radiation, GSR). The colors for the VOC species are as in Fig. 2. The DDSI for



343 each VOC species specifies the intensity of the apparent effect of drought on the decrease in BVOC emission rate during
344 the daytime, excluding DOY 306 (see Sect. 3.3).

345

346 DDSI) provides a more rigorous measure of the daytime drought effect, the PF method provides a
347 better indication of the pattern of reduced mixing ratios around noontime under drought conditions.

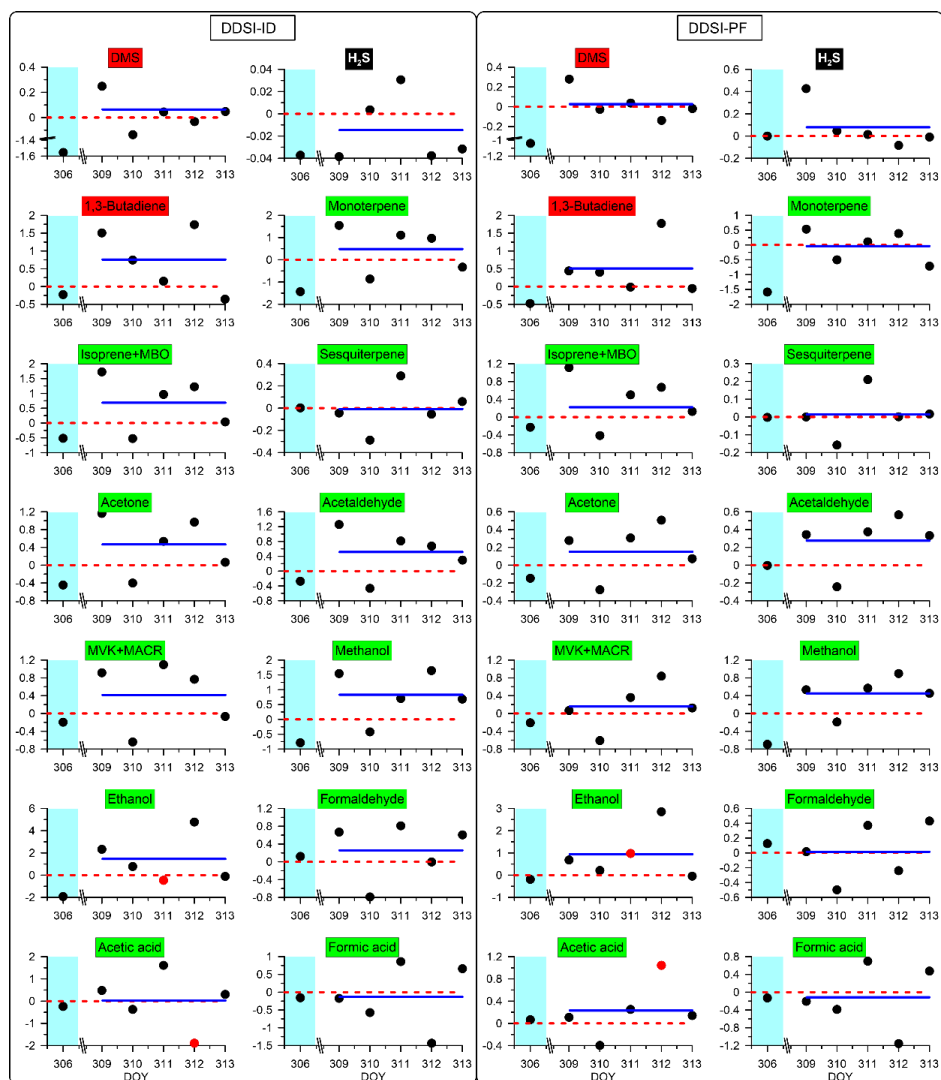
348 Figure 5 presents the DDSI values for all investigated VOCs and individually for each
349 measurement day, based on the ID approach (Eq. 1) and using the DDSI-PF approach. The ID and PF
350 approaches showed generally similar results, with a few exceptions, as explained in Sect. S3 and
351 indicated in the figure. All BVOCs showed a negative DDSI on DOY 306, except for formaldehyde
352 based on the PF method, and SQT and acetic acid, with nearly neutral DDSI, based on both methods.
353 It should be emphasized that a negative DDSI does not mean that the BVOC emissions are not affected
354 by the drought, because it is possible that with no drought effect, the calculated DDSI would be more
355 negative, reflecting the general BVOC emission enhancement with T. Hence, interpretation of the
356 drought stress on BVOC emissions in Fig. 5 should mainly focus on the trend in the DDSI following
357 the rain event on DOY 306, and in response to the day-to-day changes in meteorological conditions.

358 In general, most of the BVOCs showed a gradual increase or higher DDSI than on DOY 306,
359 during the days following DOY 306. However, this trend is masked to some extent, mostly due to the
360 negative DDSI on DOY 310 for all presumed BVOCs except ethanol. As indicated in Fig. 3, this day
361 was characterized by higher RH and lower VPD than the other investigated days, except for DOY 311.
362 However, while on the latter day, RH values remained low (below 38%), on DOY 310, RH values
363 increased sharply at around 12:00 h. Hence, the relative higher RH around noon on DOY 310
364 apparently facilitated the negative DDSI for all investigated BVOCs, except ethanol, on this day (Fig.
365 5). Negative DDSI was also observed on DOY 313 for MT and on DOY 312 for formic acid and acetic
366 acid, and to a lesser extent for formaldehyde and SQT. DOY 312 was characterized by low RH,
367 corresponding with relatively high VPD and T (Fig. 3). However, RH reached minimum values well



368 after 12:30 h on this day (Fig. 3), while remaining relatively high in the morning. This resulted in a
369 strong peak of acetic acid, formic acid, and formaldehyde at around 08:30–09:30 h (see Fig. S3),
370 followed by a later decrease of acetic acid and formic acid when RH dropped below 27%, and a later
371 decrease of formaldehyde after 14:00 h. As will be discussed below, differing from all other
372 investigated BVOCs, SQT mixing ratios reached their highest levels around noontime, corresponding
373 with low DDSI during most of the measurement days (Fig. 4).

374 Formic acid is the most soluble species among the investigated BVOCs, followed by acetic
375 acid and formaldehyde (Table 2). Figure 5 demonstrates that all three of these species corresponded
376 with negative DDSI on DOY 310. Formic acid also corresponded with negative DDSI on DOY 312,
377 whereas acetic acid and formaldehyde corresponded with negative DDSI on this day, depending on
378 the DDSI calculation method. These negative DDSIs on DOY 310 and 312 resulted from an increase
379 in their mixing ratios before noontime, along with a sharp decrease in RH (Fig. S3). This suggests that
380 those soluble species, particularly formic acid, were accumulated in the leaves at high partial pressure
381 during the day or days before being emitted in large quantities under the relatively moderate T and RH
382 before noontime of DOY 310 and DOY 312. The phenomenon of high emission rate of soluble species
383 under drought stress during relatively high RH in the morning has been demonstrated in other studies
384 (Filella et al., 2009; Loreto and Schnitzler, 2010). This further suggests that the emission of soluble
385 species is not necessarily more limited than that of non-soluble BVOCs during drought periods, as
386 long as at least low vegetation activity is maintained part of the time. This is supported by the fact that
387 pressure buildup of compounds inside the leaf can compensate for stomatal closure (Loreto and
388 Schnitzler, 2010).



389

390 **Figure 5.** Drought stress effect on BVOC mixing ratios. Presented are the DDSI values (Sect. 3.3) for DOY 306 and DOY
 391 309–313, individually for each investigated VOC, vs. DOY. Green, black, and red species names refer to presumed BVOCs,
 392 AVOCs, and either BVOCs or AVOCs, respectively. Horizontal blue and dashed red lines indicate mean and zero DDSI,
 393 respectively. Red circles indicate opposite plus/minus signs for DDSI using the ID and PF methods. These two exceptions
 394 were associated with the top 5% of the calculated standard deviation of the observed mixing ratios from the corresponding
 395 second-order polynomial fitting, which was used for the PF method.



396 Table 2 summarizes the mean DDSI for the investigated VOCs, excluding the rainy day (DOY
397 306), using the two methods, together with the VOCs' H values, scaled by color. The depletion rate of
398 the BVOC mixing ratios during the daytime due to drought stress can also be affected by chemical
399 reactions, mainly involving OH and O₃. Hence, the table also presents the rate constants of the
400 investigated VOCs with the main oxidants, OH and O₃, scaled by color, for comparison. Comparison
401 of the DDSI and these rate constants revealed no clear association between the two, suggesting a
402 relatively minor effect of the chemical reactions on the calculated DDSI values (Sect. S6). All
403 investigated BVOCs were associated with mean positive DDSI according to both methods, except for
404 SQT and formic acid, which showed either a slight negative or approximately neutral DDSI.
405 Enhancement in SQT emission under severe drought conditions, close to the wilting point, to protect
406 the plant from oxidative stress has been demonstrated (e.g., Bonn et al., 2019). While a slight negative
407 DDSI does not reflect a no-drought constraint on the BVOC emissions, the apparently more moderate
408 response to drought of the relatively more soluble species, including formic acid, acetic acid, and
409 formaldehyde (Table 2), seems to contradict the expectation of a strong stomatal response of soluble
410 BVOCs to stomatal conductance (Niinemets et al., 2004; Niinemets and Reichstein, 2003; Gabriel et
411 al., 1999). This trend results from the relatively strong response of the soluble BVOCs to higher RH
412 on DOY 310 and on DOY 312 before noon, as explained above. Among all investigated BVOCs, the
413 relatively soluble methanol and ethanol were associated with the highest DDSI values. Methanol was
414 shown to be more responsive to stomatal conductance under drought than other oxygenated BVOCs,
415 including the soluble formic acid and acetic acid (Filella et al., 2009). Interestingly, the DDSI for 1,3-
416 butadiene was relatively high. While 1,3-butadiene is frequently used as a proxy for anthropogenic
417 emissions (e.g., Chang et al., 2014; Khan et al., 2018; Lewandowski et al., 2015), there are indications
418 of this species' emission from biogenic origin as well. Huang et al. (2020) reported emission of 1,3-
419 butadiene in dynamic chamber experiments from both soil and leaves, somewhat higher for the former.



420 Asensio et al. (2007) also reported a high emission rate compared to other BVOCs. Thus, emission of
 421 1,3-butadiene from both the soil and vegetation might have contributed to its observed mixing ratios.

422

423 **Table 2.** Henry's law constant (H), calculated DDSI for the daytime on DOY 306 and DOY 309–313, and oxidation rate
 424 constant of each VOC species. Mean DDSI values for the investigated VOCs, evaluated based on the ID and PF methods
 425 (Sect. 3.3), are presented, with red, blue, and no shading indicating positive, negative, and approximately neutral DDSI,
 426 respectively. The rate constants of each VOC with OH and O₃ are also presented, individually scaled on a normalized
 427 white–red scale.

	Henry's law constant for solubility in water at 298.15 K (mol m ⁻³ Pa ⁻¹)	DDSI-ID	DDSI-PF	OH rate constant at 25°C (cm ³ molecule ⁻¹ s ⁻¹)	O ₃ rate constant at 25°C (cm ³ molecule ⁻¹ s ⁻¹)
Isoprene	1.29E-04 ^a	0.686	0.221	9.99E-11	1.28E-17
MT *	1.68E-04 ^{a+b}	0.485	-0.038	1.36E-10	1.08E-16
SQT *	3.54E-04 ^c	-0.007	0.014	2.44E-10	1.20E-14
Acetone	2.58E-01 ^a	0.466	0.152	1.75E-13	
Acetaldehyde	1.43E-01 ^a	0.515	0.275	1.49E-11	
MVK **	2.60E-01 ^b	0.415	0.155	1.88E-11	
Methanol	2.17E+00 ^a	0.833	0.452	8.96E-13	
Ethanol	1.97E+00 ^a	1.460	0.936	3.21E-12	
Formaldehyde	3.28E+01 ^a	0.257	0.016	8.49E-12	
Acetic acid	7.52E+01 ^a	0.026	0.230	7.40E-13	
Formic acid	5.93E+03 ^a	-0.131	-0.115	4.50E-13	
DMS	5.60E-03 ^b	0.034	0.027	4.84E-12	
H ₂ S	1.00E-03 ^b	-0.015	0.079	4.80E-12	
1,3-Butadiene	1.00E-04 ^b	0.758	0.509	6.65E-11	6.33E-18

428

429 *The rate constants for MTs are averaged values of α-pinene, β-pinene, limonene, D-limonene, and myrcene, and for SQTs,
 430 averaged values of α-farnesene, β-caryophyllene, and humulene. The H value for MT was based on the relative emission
 431 rates of myrcene, sabinene, limonene, 3-carene, t-β-ocimene, α-pinene, and β-pinene (together accounting for 93% of the
 432 total MTs, according the MEGAN model); while the H value for SQT was based on the relative emission rates of α-
 433 farnesene and β-caryophyllene (together accounting for 38% of the total SQTs in MEGAN).

434 **The H value and OH/O₃ rate constants are for MVK only, while the DDSI-ID and DDSI-PF values are for MVK +
 435 MACR.

436 a. (Niinemets and Reichstein, 2003); b. (Sander, 2023); c. (Copolovici and Niinemets, 2015).



437 ***3.4 Meteorological parameters as a proxy for variations in BVOC mixing ratio under drought***
438 ***conditions***

439 To investigate the effect of meteorological parameters on BVOC mixing ratios, we tested the
440 correlation of the investigated VOC mixing ratios to RH, T, GSR and VPD. Table 3 shows the Pearson
441 correlation coefficient (R) between these meteorological parameters and the measured mixing ratios
442 of the various investigated VOCs, during the daytime of the investigated periods (DOY 306 and DOY
443 309–313). Considering that the rain event on DOY 306 could significantly affect the results, we also
444 present the corresponding R values for the same period, excluding DOY 306. To further focus the
445 analysis on the drought effect, we repeated it with exclusion of the early morning measurements
446 (before 08:30 h) as well, considering the relatively high RH values during the early morning. We chose
447 08:30 h because most of the BVOC species showed an increase in concentration before this time point,
448 as would be expected for increases in T and GSR under drought conditions when RH is relatively high
449 (Filella et al., 2009; Loreto and Schnitzler, 2010). Finally, for the same reason, we also excluded the
450 late afternoon (later than 15:30 h), when a less severe drought effect is expected.

451 Table 3 suggests that GSR is the best proxy for the effect of drought on the BVOC mixing
452 ratios. Whereas under non-drought conditions, a positive correlation between solar radiation and
453 BVOC emissions is expected (Staudt et al., 2000; Guenther et al., 1995), Table 3 demonstrates a
454 negative R for all BVOCs with GSR, except for SQT. The anticorrelation tended to be stronger when
455 calculated after 08:30 h, and to a lesser extent between 08:30 and 15:30 h. The lower correlation of
456 RH and T, compared to GSR, with the BVOC mixing ratios may arise from the fact that under severe
457 drought, the effect of RH may tend to be a dominant factor in restricting BVOC emissions, whereas
458 under less severe drought, T tends to enhance BVOC emissions (Sect. 1). Therefore, because of the



459 general anticorrelation between RH and T, neither shows a dominant impact on the BVOC mixing
 460 ratios when calculated over the whole investigation period.

461 Interestingly, 1,3-butadiene showed a very high correlation with RH. This may reinforce our
 462 previous assumption that it is emitted from a biogenic origin, such as the soil or vegetation, at the
 463 measurement site. According to Asensio et al. (2007), an increase in soil temperature above 25 °C can
 464 lead to a significant decrease in 1,3-butadiene emission; during our measurements, the soil temperature
 465 probably reached higher values during most of the daytime. Because soil temperature tends to
 466 anticorrelate with atmospheric RH, a decrease in RH during the daytime can be expected to result in a
 467 decrease in 1,3-butadiene emission rates. This may be further indicated by the higher correlation of
 468 1,3-butadiene with RH when the morning period is excluded (see Table 3).

469

470 **Table 3.** Pearson correlation coefficient (R) for the correlation between the quantified VOCs’ mixing ratios and RH, T,
 471 GSR, and VPD during the daytime of DOY 306 and DOY 309–313. The values are also presented for the same period,
 472 excluding measurements before 08:30 h, and before 08:30 and after 15:30 h.

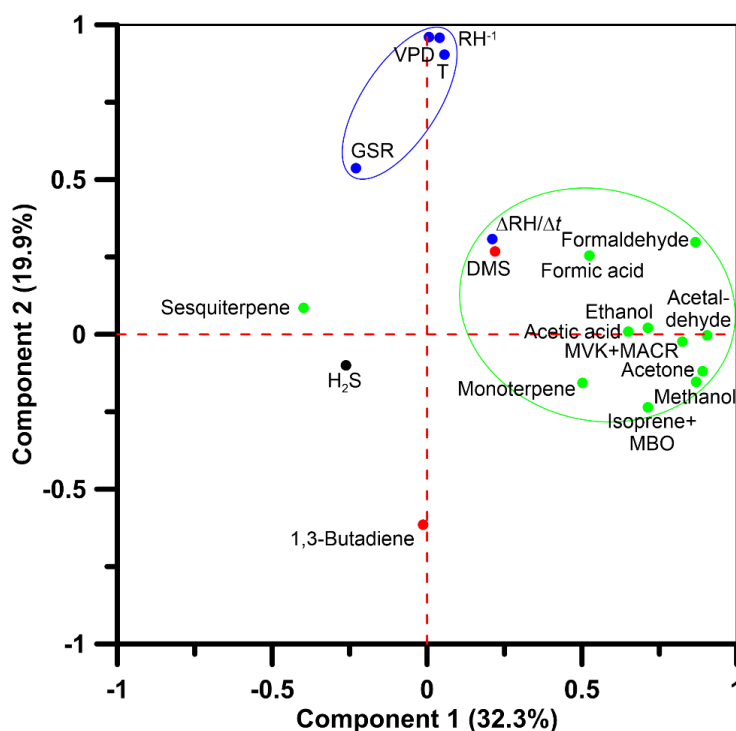
VOCs	All measurement days				Without the rainy day (DOY 306)				After 08:30 h and without the rainy day (DOY 306)				Between 08:30 h and 15:30 h, without the rainy day (DOY 306)			
	R(RH)	R(T)	R(GSR)	R(VPD)	R(RH)	R(T)	R(GSR)	R(VPD)	R(RH)	R(T)	R(GSR)	R(VPD)	R(RH)	R(T)	R(GSR)	R(VPD)
DMS	-0.271	0.092	0.070	0.254	-0.247	0.070	-0.067	0.225	-0.314	0.112	-0.242	0.234	-0.326	0.154	-0.227	0.262
MT	0.216	-0.014	-0.205	-0.166	0.024	-0.068	-0.224	-0.011	-0.263	0.371	-0.185	0.346	-0.278	0.517	-0.148	0.432
Acetone	0.019	-0.018	-0.163	-0.034	0.081	-0.015	-0.242	-0.086	0.055	0.013	-0.301	-0.024	0.082	0.048	-0.269	-0.021
Isoprene+MBO	0.395	-0.059	-0.188	-0.367	0.151	-0.103	-0.121	-0.191	0.242	-0.101	-0.155	-0.193	0.309	-0.098	-0.101	-0.228
Acetaldehyde	-0.067	0.021	-0.027	0.025	-0.048	0.033	-0.071	0.002	0.040	-0.042	-0.131	-0.027	0.093	-0.040	-0.071	-0.049
MVK+MACR	0.086	0.118	-0.086	-0.075	-0.004	0.111	-0.063	-0.005	0.142	-0.035	-0.176	-0.097	0.170	-0.023	-0.145	-0.105
H ₂ S	-0.043	-0.239	0.061	-0.064	0.028	-0.239	0.038	-0.130	-0.022	-0.036	0.354	-0.006	-0.047	-0.097	0.327	-0.020
1,3-Butadiene	0.665	-0.123	-0.121	-0.569	0.612	-0.300	-0.026	-0.545	0.730	-0.470	0.020	-0.642	0.735	-0.473	0.054	-0.647
SQT	-0.073	-0.011	0.237	0.020	-0.064	-0.008	0.245	0.006	0.067	-0.082	0.298	-0.077	0.041	-0.154	0.265	-0.096
Methanol	0.187	-0.124	-0.219	-0.220	0.046	-0.179	-0.305	-0.133	-0.083	-0.013	-0.289	0.045	-0.074	0.055	-0.214	0.078
Ethanol	-0.068	0.006	-0.198	0.048	-0.047	0.013	-0.227	0.030	-0.074	-0.020	-0.289	0.031	-0.071	0.029	-0.241	0.053
Formaldehyde	-0.395	0.178	-0.026	0.319	-0.291	0.204	-0.097	0.224	-0.127	-0.004	-0.264	0.067	-0.103	0.012	-0.248	0.064
Acetic acid	-0.039	0.059	-0.037	-0.003	0.017	0.065	-0.049	-0.051	0.357	-0.295	-0.162	-0.316	0.387	-0.307	-0.151	-0.334
Formic acid	-0.160	0.266	-0.048	0.109	-0.170	0.260	-0.036	0.109	0.360	-0.301	-0.286	-0.357	0.378	-0.295	-0.280	-0.364

473

474 We further hypothesized that the intensity of the instantaneous intraday variations in the
 475 meteorological parameters may play a role in the BVOC emissions, and therefore can be used as a



476 proxy for BVOC emissions, rather than the values of the meteorological parameters themselves. To
 477 test this, Fig. S4 presents a principal component analysis (PCA) (Wold et al., 1987) for all investigated
 478 VOCs, T, RH, VPD, and GSR, as well as the linear regression slope coefficients of these
 479 meteorological parameters ($\frac{\Delta T}{\Delta t}$, $\frac{\Delta RH}{\Delta t}$, $\frac{\Delta VPD}{\Delta t}$, $\frac{\Delta GSR}{\Delta t}$, respectively); Fig. 6 presents a PCA for the same
 480 parameters, excluding $\frac{\Delta T}{\Delta t}$, $\frac{\Delta VPD}{\Delta t}$ and $\frac{\Delta GSR}{\Delta t}$. Both figures demonstrate that $\frac{\Delta RH}{\Delta t}$ has the highest
 481 association with the BVOC mixing ratios; this is more clearly demonstrated in Fig. 6. This figure
 482 clearly indicates that all BVOCs except SQT correlated with component 1 (32.3%) together with $\frac{\Delta RH}{\Delta t}$,



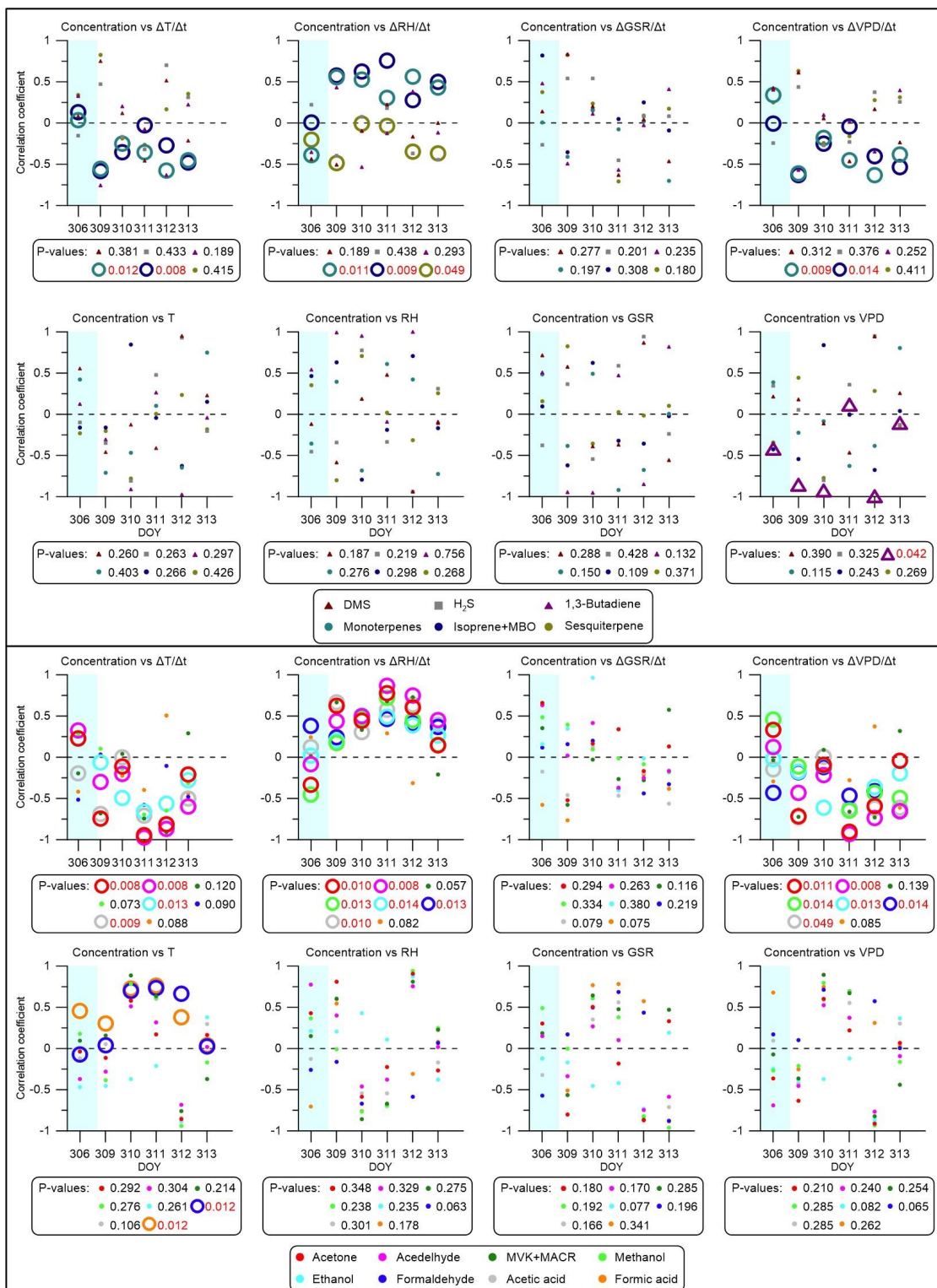
493 **Figure 6.** PCA of ambient meteorological parameters, including meteorological parameters and the temporal derivative of
 494 RH, and the measured mixing ratios of VOCs. Colors indicate ambient meteorological parameters (blue), BVOCs (green),
 495 AVOCs (black), and either BVOCs or AVOCs (red). Note that the inverse of RH is presented rather than RH.



496 indicating a dominant role for $\frac{\Delta RH}{\Delta t}$ in the BVOC mixing ratios, rather than any of the meteorological
497 parameters. The weak correlation of SQT with $\frac{\Delta RH}{\Delta t}$ may result from this species' tendency to be
498 emitted at a higher rate close to the wilting point, as suggested by Bonn et al. (2019).

499 The effect of meteorological conditions on the rate of BVOC emissions is expected to show
500 day-to-day variations, particularly for this specific study, considering the relief in drought stress on
501 DOY 306 and 310 and before noontime on DOY 312. To investigate the response of the mixing ratios
502 to meteorological parameters on a daily basis, we evaluated the regression coefficient for the mixing
503 ratios vs. each of T, RH, GSR, and VPD, as well as their temporal derivatives
504 ($\frac{\Delta T}{\Delta t}$, $\frac{\Delta RH}{\Delta t}$, $\frac{\Delta GSR}{\Delta t}$, $\frac{\Delta VPD}{\Delta t}$, respectively), individually for each measurement day. Figure 7 shows the 30-
505 min-based Pearson correlation coefficients (PCC(R)) for the investigated VOCs, separately for each
506 day and individually for soluble ($H > 0.1$) and insoluble ($H < 0.1$) species (Murphy and Morrison,
507 2014).

508 The figure demonstrates a higher correlation for BVOC mixing ratios with the instantaneous
509 change in the meteorological parameters, than with the meteorological parameters themselves.
510 Exceptional is $\frac{\Delta GSR}{\Delta t}$, which appears, similar to GSR, to be a poor proxy for BVOC emissions. This
511 reinforces the notion that the apparently dominant role played by GSR in the BVOCs' emission (see
512 Table 3) results only from the fact that RH and T tend to anticorrelate and cancel out each other's
513 effects during the measurements, as explained above. Figure 7 further emphasizes the important role
514 of the temporal gradient of the tested meteorological parameters, particularly $\frac{\Delta RH}{\Delta t}$, in the emission of
515 BVOCs under drought conditions, which was also captured without performing the analysis on a daily
516 basis (Fig. 6).





518 **Figure 7.** Daytime correlation coefficient between mixing ratios and meteorological parameters and their temporal
519 derivatives for relatively non-soluble (upper panel) and soluble (lower panel) VOCs (see H values in Table 2). The colors
520 of the symbols are unique to each VOC species. Circles represent presumed BVOCs, squares represent presumed AVOC
521 (H_2S), and triangles represent either BVOCs or AVOCs, including DMS and 1,3-butadiene. Large empty symbols and
522 values in red indicate statistically significant correlations ($P < 0.05$), with P -values calculated excluding measurements on
523 the rainy day (DOY 306); blue shaded rectangle indicates rain event.

524 Table 4 summarizes the results shown in Fig. 7 and indicates, individually for each VOC,
525 whether any of the correlation types presented in Fig. 7 are statistically significant, based on the null
526 hypothesis of $R = 0$ ($P < 0.05$) using a one-sample t-test. The P -value calculation was based on the
527 DOY 309–313 data, excluding DOY 306 during which a rain event occurred.

528 Overall, Table 4 clearly indicates that the temporal gradients of the meteorological parameters
529 correspond with a much higher number of cases (23 out of 26) for which the correlation or
530 anticorrelation with the BVOC mixing ratios were found to be statistically significant, compared to
531 the meteorological parameters themselves (3 out of 26). Out of these 23 cases, the anticorrelation of
532 SQT with $\frac{\Delta RH}{\Delta t}$ is exceptional, reflecting an increase in its emission rate with increasing drought stress,
533 in agreement with the analysis presented in Table 3. Table 4 suggests that under the studied
534 conditions, $\frac{\Delta RH}{\Delta t}$ is the best proxy for the emission of BVOCs under drought stress. The ranking for the
535 various tested meteorological parameters serving as good predictors for BVOC emission rates under
536 drought conditions is as follows: $\frac{\Delta RH}{\Delta t} > \frac{\Delta VPD}{\Delta t} > \frac{\Delta T}{\Delta t} > T > VPD > \frac{\Delta GSR}{\Delta t} > GSR = RH$.

537 There was no significant difference in the results for the soluble vs. non-soluble BVOCs.
538 However, both formaldehyde and formic acid, which are among the most soluble BVOCs included in
539 our study (see Table 2), corresponded with a significant correlation ($P < 0.05$) with T, while among
540 these two species, only formaldehyde also showed a significant correlation with $\frac{\Delta RH}{\Delta t}$. These results
541 are in line with our previous findings that relatively elevated RH during periods of drought stress can



542 enhance the emission rate of soluble BVOCs with increasing T, as was demonstrated for DOY 306
 543 and 310, and for DOY 312 before noon (Sect. 3.3).

544 The statistically significant anticorrelation of SQT mixing ratios with $\frac{\Delta RH}{\Delta t}$ under drought
 545 conditions may agree with Bonn et al. (2019), who found that a sharp increase in SQT emission occurs
 546 close to the wilting point, apparently to protect the plant against oxidative damage. The increase in
 547 SQT emission rate in response to drought stress is further supported by Caser et al. (2019), who found
 548 that drought can induce the mechanism of SQT synthesis.

549

550 **Table 4.** Correlation of the investigated VOCs with various meteorological parameters. Presented is the number of VOCs
 551 for which a non-statistically significant and statistically significant R with various meteorological conditions and their
 552 temporal derivatives ($\frac{\Delta T}{\Delta t}$, $\frac{\Delta RH}{\Delta t}$, $\frac{\Delta VPD}{\Delta t}$, $\frac{\Delta GSR}{\Delta t}$ and $\frac{\Delta RH}{\Delta t}$ are the temporal derivatives of T, RH, VPD, GSR and RH, respectively)
 553 was observed. Red and blue shading indicate positive and negative correlation, respectively. Darker color (red or blue)
 554 indicates statistically significant correlation ($P < 0.05$), while light color indicates a non-statistically significant correlation,
 555 with $0.1 > P > 0.05$.

556

557

558

559

560

561

562

563

564

565

566

567

568

569

570

571

	<i>T</i>	$\frac{\Delta T}{\Delta t}$	<i>RH</i>	$\frac{\Delta RH}{\Delta t}$	<i>VPD</i>	$\frac{\Delta VPD}{\Delta t}$	<i>GSR</i>	$\frac{\Delta GSR}{\Delta t}$
DMS								
H₂S								
1,3-Butadiene								
MT								
Isoprene+MBO								
SQT								
Acetone								
Acetaldehyde								
MVK+MACR								
Methanol								
Ethanol								
Formaldehyde								
Acetic acid								
Formic acid								
	2	6+3	1	8+2+1	2+1	8+1	1	2



572 4. Summary and conclusions

573 We investigated the effect of meteorological conditions on BVOC mixing ratios under drought. Under
574 the drought conditions in this study, the instantaneous changes in meteorological conditions,
575 $\frac{\Delta RH}{\Delta t}$, $\frac{\Delta VPD}{\Delta t}$ and $\frac{\Delta T}{\Delta t}$, were found to be better proxies for the mixing ratios of the investigated BVOCs at
576 the canopy scale than the absolute values of RH, T, VPD and GSR. In particular, $\frac{\Delta RH}{\Delta t}$ was associated
577 with a positive correlation for 10 out of 11 of the investigated presumed BVOCs. These findings are
578 consistent with those presented in the companion paper by Li et al. (2023), which is based on direct
579 flux measurements from branches of natural vegetation in the same region. For 8 out of the 11
580 investigated VOCs, a statistically significant positive correlation was observed between $\frac{\Delta RH}{\Delta t}$ and the
581 BVOC mixing ratios. SQT showed an anticorrelation with $\frac{\Delta RH}{\Delta t}$, in line with previous studies indicating
582 an increase in its emission rate under severe drought conditions, close to the wilting point.

583 Our analyses reinforce previous studies indicating enhanced emission rates of soluble species
584 under higher RH during drought periods, including formaldehyde, formic acid, and acetic acid,
585 resulting in a lower DDSI than for the non-soluble BVOCs. Moreover, formic acid and formaldehyde
586 showed a significant positive correlation with T in the daily-basis analysis; the latter also showed a
587 significant positive correlation with $\frac{\Delta RH}{\Delta t}$. The dramatic effect of relatively high RH during a drought
588 period emphasizes the need to analyze the results on a timescale of 1 day or less, for cases in which
589 significant day-to-day or intraday changes in meteorological conditions occur. Moreover, applying the
590 analysis to the whole investigation period, rather than on a daily scale, resulted in GSR being the best
591 proxy for most of the BVOC mixing ratios, with a negative correlation to them. This resulted from the
592 large changes in RH during the drought period, leading to opposite effects of RH and T, which tend to
593 be anticorrelated, on BVOC emissions. Namely, under high RH, BVOC emission rates could increase



594 with increasing T, whereas under low RH, the BVOC emission rates decreased with increasing T and
595 decreasing RH.

596 The strong correlation of 1,3-butadiene with RH, when calculated over the whole campaign
597 period during the daytime (see Table 3), reinforces findings from previous studies indicating a biogenic
598 source for this compound, from both vegetation and soil. Considering the frequent use of 1,3-butadiene
599 as a proxy for anthropogenic emissions, such studies should take into account its potentially significant
600 biogenic emission.

601 Overall, our study aligns with previous findings on the effect of drought on BVOC emission
602 rates. Notably, we revealed that instantaneous changes in meteorological conditions may serve as a
603 more adequate proxy for BVOC emissions during drought than the absolute values of those parameters.
604 These insights are highly relevant for the enhancement of air quality and climate models. However, it
605 is important to note that the present study did not thoroughly investigate the impact of chemical loss
606 and changes in mixing layer height on BVOC mixing ratios. Similarly, the study conducted by Li et
607 al. (2023), which led to similar findings based on direct flux measurements, did not assess the influence
608 of drought on BVOCs at the ecosystem level. Therefore, additional research is needed to better
609 understand the effects of instantaneous changes in meteorological conditions on BVOC emissions, and
610 how these affect BVOC concentration at the canopy level.

611

612 **Author contribution.** ET designed the experiments, MG carried out the field measurements and
613 performed the data acquisition together with CD. PM and EF led the calibration, quality control, and
614 data processing. AG set up the MEGANv2.1 model. QL and ET led the analyses with contributions
615 from all co-authors. QL and ET prepared the manuscript with contributions from AG.

616

617 **Competing interests.** The authors declare that they have no conflict of interest.



618 Acknowledgements

619 We want to greatly thank Gil Lerner for supporting the measurements. This study was supported by
620 the Israel Science Foundation, Grant Nos. 1787/15 and 543/22. Eran Tas holds the Joseph H. and
621 Belle R. Braun Senior Lectureship in Agriculture.

622 References

- 623 Asensio, D., Peñuelas, J., Llusà, J., Ogaya, R., and Filella, I.: Interannual and interseasonal soil CO₂ efflux and
624 VOC exchange rates in a Mediterranean holm oak forest in response to experimental drought, *Soil Biology
625 and Biochemistry*, 39, 2471–2484, doi:10.1016/j.soilbio.2007.04.019, 2007.
- 626 Baldwin, I. T., Halitschke, R., Paschold, A., Dahl, C. C. von, and Preston, C. A.: Volatile signaling in plant-plant
627 interactions: "talking trees" in the genomics era, *Science (New York, N.Y.)*, 311, 812–815,
628 doi:10.1126/science.1118446, 2006.
- 629 Berg, A. R., Heald, C. L., Huff Hartz, K. E., Hallar, A. G., Meddens, A. J. H., Hicke, J. A., Lamarque, J.-F., and Tilmes,
630 S.: The impact of bark beetle infestations on monoterpene emissions and secondary organic aerosol
631 formation in western North America, *Atmos. Chem. Phys.*, 13, 3149–3161, doi:10.5194/acp-13-3149-2013,
632 2013.
- 633 Blande, J. D., Tiiva, P., OKSANEN, E., and Holopainen, J. K.: Emission of herbivore-induced volatile terpenoids
634 from two hybrid aspen (*Populus tremula* × *tremuloides*) clones under ambient and elevated ozone
635 concentrations in the field, *Glob Change Biol*, 13, 2538–2550, doi:10.1111/j.1365-2486.2007.01453.x,
636 2007.
- 637 Bonn, B., Magh, R.-K., Rombach, J., and Kreuzwieser, J.: Biogenic isoprenoid emissions under drought stress:
638 Different responses for isoprene and terpenes, *Biogeosciences*, 16, 4627–4645, doi:10.5194/bg-16-4627-
639 2019, 2019.
- 640 Bourtsoukidis, E., Kawaletz, H., Radacki, D., Schütz, S., Hakola, H., Hellén, H., Noe, S., Mölder, I., Ammer, C.,
641 and Bonn, B.: Impact of flooding and drought conditions on the emission of volatile organic compounds of
642 *Quercus robur* and *Prunus serotina*, *Trees*, 28, 193–204, doi:10.1007/s00468-013-0942-5, 2014.
- 643 Brilli, F., Barta, C., Fortunati, A., Lerda, M., Loreto, F., and Centritto, M.: Response of isoprene emission and
644 carbon metabolism to drought in white poplar (*Populus alba*) saplings, *New Phytol*, 175, 244–254,
645 doi:10.1111/j.1469-8137.2007.02094.x, 2007.
- 646 Brilli, F., Ciccioli, P., Frattoni, M., Prestininzi, M., Spanedda, A. F., and Loreto, F.: Constitutive and herbivore-
647 induced monoterpenes emitted by *Populus x euroamericana* leaves are key volatiles that orient
648 *Chrysomela populi* beetles, *Plant, cell & environment*, 32, 542–552, doi:10.1111/j.1365-
649 3040.2009.01948.x, 2009.
- 650 Calfapietra, C., Fares, S., Manes, F., Morani, A., Sgrigna, G., and Loreto, F.: Role of Biogenic Volatile Organic
651 Compounds (BVOC) emitted by urban trees on ozone concentration in cities: A review, *Environmental
652 pollution (Barking, Essex 1987)*, 183, 71–80, doi:10.1016/j.envpol.2013.03.012, 2013.
- 653 Caser, M., Chitarra, W., D'Angiolillo, F., Perrone, I., Demasi, S., Lovisolo, C., Pistelli, L., Pistelli, L., and Scariot,
654 V.: Drought stress adaptation modulates plant secondary metabolite production in *Salvia dolomitica* Codd,
655 *Industrial Crops and Products*, 129, 85–96, doi:10.1016/j.indcrop.2018.11.068, 2019.



- 656 Chamberlain, A.C. and Chadwick, R.C.: Deposition of airborne radioiodine vapor, *Health and Environmental*
657 *Research*, 8, 22–25, 1953.
- 658 Chang, C.-C., Wang, J.-L., Candice Lung, S.-C., Chang, C.-Y., Lee, P.-J., Chew, C., Liao, W.-C., Chen, W.-N., and
659 Ou-Yang, C.-F.: Seasonal characteristics of biogenic and anthropogenic isoprene in tropical–subtropical
660 urban environments, *Atmospheric Environment*, 99, 298–308, doi:10.1016/j.atmosenv.2014.09.019, 2014.
- 661 Cook, B. I., Anchukaitis, K. J., Touchan, R., Meko, D. M., and Cook, E. R.: Spatiotemporal drought variability in
662 the Mediterranean over the last 900 years, *Journal of geophysical research. Atmospheres JGR*, 121, 2060–
663 2074, doi:10.1002/2015jd023929, 2016.
- 664 Copolovici, L. and Niinemets, Ü.: Temperature dependencies of Henry's law constants for different plant
665 sesquiterpenes, *Chemosphere*, 138, 751–757, doi:10.1016/j.chemosphere.2015.07.075, 2015.
- 666 Curci, G., Beekmann, M., Vautard, R., Smiatek, G., Steinbrecher, R., Theloke, J., and Friedrich, R.: Modelling
667 study of the impact of isoprene and terpene biogenic emissions on European ozone levels, *Atmospheric*
668 *Environment*, 43, 1444–1455, doi:10.1016/j.atmosenv.2008.02.070, 2009.
- 669 Dayan, C., Fredj, E., Misztal, P. K., Gabay, M., Guenther, A. B., and Tas, E.: Emission of biogenic volatile organic
670 compounds from warm and oligotrophic seawater in the Eastern Mediterranean, *Atmos. Chem. Phys.*, 20,
671 12741–12759, doi:10.5194/acp-20-12741-2020, 2020.
- 672 Derimian, Y., Choël, M., Rudich, Y., Deboudt, K., Dubovik, O., Laskin, A., Legrand, M., Damiri, B., Koren, I., Unga,
673 F., Moreau, M., Andreae, M. O., and Karnieli, A.: Effect of sea breeze circulation on aerosol mixing state
674 and radiative properties in a desert setting, *Atmos. Chem. Phys.*, 17, 11331–11353, doi:10.5194/acp-17-
675 11331-2017, 2017.
- 676 Filella, I., Peñuelas, J., and Seco, R.: Short-chained oxygenated VOC emissions in *Pinus halepensis* in response
677 to changes in water availability, *Acta Physiol Plant*, 31, 311–318, doi:10.1007/s11738-008-0235-6, 2009.
- 678 Filella, I., Primante, C., Llusià, J., Martín González, A. M., Seco, R., Farré-Armengol, G., Rodrigo, A., Bosch, J.,
679 and Peñuelas, J.: Floral advertisement scent in a changing plant-pollinators market, *Scientific reports*, 3,
680 3434, doi:10.1038/srep03434, 2013.
- 681 Fortunati, A., Barta, C., Brilli, F., Centritto, M., Zimmer, I., Schnitzler, J.-P., and Loreto, F.: Isoprene emission is
682 not temperature-dependent during and after severe drought-stress: A physiological and biochemical
683 analysis, *The Plant journal for cell and molecular biology*, 55, 687–697, doi:10.1111/j.1365-
684 313X.2008.03538.x, 2008.
- 685 Gabriel, R., Schäfer, L., Gerlach, C., Rausch, T., and Kesselmeier, J.: Factors controlling the emissions of volatile
686 organic acids from leaves of *Quercus ilex* L. (Holm oak), *Atmospheric Environment*, 33, 1347–1355,
687 doi:10.1016/S1352-2310(98)00369-0, 1999.
- 688 Giorgi, F.: Climate change hot - spots, *Geophys. Res. Lett.*, 33, 739, doi:10.1029/2006gl025734, 2006.
- 689 Goldstein, A. H., McKay, M., Kurpius, M. R., Schade, G. W., Lee, A., Holzinger, R., and Rasmussen, R. A.: Forest
690 thinning experiment confirms ozone deposition to forest canopy is dominated by reaction with biogenic
691 VOCs, *Geophys. Res. Lett.*, 31, 22,123, doi:10.1029/2004GL021259, 2004.
- 692 Graus, M., Müller, M., and Hansel, A.: High resolution PTR-TOF: Quantification and formula confirmation of
693 VOC in real time, *Journal of the American Society for Mass Spectrometry*, 21, 1037–1044,
694 doi:10.1016/j.jasms.2010.02.006, 2010.
- 695 Guenther, A., Hewitt, C. N., Erickson, D., Fall, R., Geron, C., Graedel, T., Harley, P., Klinger, L., Lerdau, M., McKay,
696 W. A., Pierce, T., Scholes, B., Steinbrecher, R., Tallamraju, R., Taylor, J., and Zimmerman, P.: A global model
697 of natural volatile organic compound emissions, *J. Geophys. Res.*, 100, 8873–8892, 1995.



- 698 Guenther, A. B., Jiang, X., Heald, C. L., Sakulyanontvittaya, T., Duhl, T., Emmons, L. K., and Wang, X.: The Model
699 of Emissions of Gases and Aerosols from Nature version 2.1 (MEGAN2.1): An extended and updated
700 framework for modeling biogenic emissions, *Geosci. Model Dev.*, 5, 1471–1492, doi:10.5194/gmd-5-1471-
701 2012, 2012.
- 702 Hansen, U. and Seufert, G.: Terpenoid emission from citrus sinensis (L.) OSBECK under drought stress, *Physics
703 and Chemistry of the Earth, Part B: Hydrology, Oceans and Atmosphere*, 24, 681–687, doi:10.1016/S1464-
704 1909(99)00065-9, 1999.
- 705 Harley, P. C.: The Roles of Stomatal Conductance and Compound Volatility in Controlling the Emission of
706 Volatile Organic Compounds from Leaves, in: *Biology, Controls and Models of Tree Volatile Organic
707 Compound Emissions*, Niinemets, Ü., and Monson, R. K. (Eds.), Springer Netherlands, Dordrecht, 181–208,
708 2013.
- 709 Harper, K. L. and Unger, N.: Global climate forcing driven by altered BVOC fluxes from 1990 to 2010 land cover
710 change in maritime Southeast Asia, *Atmos. Chem. Phys.*, 18, 16931–16952, doi:10.5194/acp-18-16931-
711 2018, 2018.
- 712 Hoerling, M., Eischeid, J., Perlwitz, J., Quan, X., Zhang, T., and Pegion, P.: On the Increased Frequency of
713 Mediterranean Drought, *Journal of Climate*, 25, 2146–2161, doi:10.1175/JCLI-D-11-00296.1, 2012.
- 714 Holopainen, J. K. and Gershenson, J.: Multiple stress factors and the emission of plant VOCs, *Trends in plant
715 science*, 15, 176–184, doi:10.1016/j.tplants.2010.01.006, 2010.
- 716 Holzinger, R.: PTRwid: A new widget tool for processing PTR-TOF-MS data, *Atmos. Meas. Tech.*, 8, 3903–3922,
717 doi:10.5194/amt-8-3903-2015, 2015.
- 718 Huang, X., Lai, J., Liu, Y., Zheng, L., Fang, X., Song, W., and Yi, Z.: Biogenic volatile organic compound emissions
719 from *Pinus massoniana* and *Schima superba* seedlings: Their responses to foliar and soil application of
720 nitrogen, *The Science of the total environment*, 705, 135761, doi:10.1016/j.scitotenv.2019.135761, 2020.
- 721 IPCC: *Climate Change 2007: Impacts, Adaptation and Vulnerability*, Intergovernmental Panel on Climate
722 Change (IPCC), Cambridge University Press, Cambridge, UK, 976 pp., 2007.
- 723 Janson, R. and Serves, C. de: Acetone and monoterpene emissions from the boreal forest in northern Europe,
724 *Atmospheric Environment*, 35, 4629–4637, doi:10.1016/S1352-2310(01)00160-1, 2001.
- 725 Jordan, A., Haidacher, S., Hanel, G., Hartungen, E., Herbig, J., Märk, L., Schottkowsky, R., Seehauser, H., Sulzer,
726 P., and Märk, T. D.: An online ultra-high sensitivity Proton-transfer-reaction mass-spectrometer combined
727 with switchable reagent ion capability (PTR+SRI-MS), *International Journal of Mass Spectrometry*, 286,
728 32–38, doi:10.1016/j.ijms.2009.06.006, 2009.
- 729 Kanda, K.-i. and Tsuruta, H.: Emissions of sulfur gases from various types of terrestrial higher plants, *Soil
730 Science and Plant Nutrition*, 41, 321–328, doi:10.1080/00380768.1995.10419589, 1995.
- 731 Karl, T., Guenther, A., Spirig, C., Hansel, A., and Fall, R.: Seasonal variation of biogenic VOC emissions above a
732 mixed hardwood forest in northern Michigan, *Geophys. Res. Lett.*, 30, doi:10.1029/2003gl018432, 2003.
- 733 Khan, M., Schlich, B.-L., Jenkin, M., Shallcross, B., Moseley, K., Walker, C., Morris, W., Derwent, R., Percival, C.,
734 and Shallcross, D.: A Two-Decade Anthropogenic and Biogenic Isoprene Emissions Study in a London Urban
735 Background and a London Urban Traffic Site, *Atmosphere*, 9, 387, doi:10.3390/atmos9100387, 2018.
- 736 Knighton, W. B., Fortner, E. C., Herndon, S. C., Wood, E. C., and Miake-Lye, R. C.: Adaptation of a proton
737 transfer reaction mass spectrometer instrument to employ NO⁺ as reagent ion for the detection of 1,3-
738 butadiene in the ambient atmosphere, *Rapid communications in mass spectrometry RCM*, 23, 3301–3308,
739 doi:10.1002/rcm.4249, 2009.



- 740 Kreuzwieser, J., Meischner, M., Grün, M., Yáñez-Serrano, A. M., Fasbender, L., and Werner, C.: Drought affects
741 carbon partitioning into volatile organic compound biosynthesis in Scots pine needles, *New Phytol*, 232,
742 1930–1943, doi:10.1111/nph.17736, 2021.
- 743 Lelieveld, J., Hadjinicolaou, P., Kostopoulou, E., Chenoweth, J., El Maayar, M., Giannakopoulos, C., Hannides,
744 C., Lange, M. A., Tanarhte, M., Tyrllis, E., and Xoplaki, E.: Climate change and impacts in the Eastern
745 Mediterranean and the Middle East, *Climatic change*, 114, 667–687, doi:10.1007/s10584-012-0418-4,
746 2012.
- 747 Lewandowski, M., Jaoui, M., Offenber, J. H., Krug, J. D., and Kleindienst, T. E.: Atmospheric oxidation of
748 isoprene and 1,3-butadiene: Influence of aerosol acidity and relative humidity on secondary organic
749 aerosol, *Atmos. Chem. Phys.*, 15, 3773–3783, doi:10.5194/acp-15-3773-2015, 2015.
- 750 Li, Q., Gabay, M., Rubin, Y., Raveh-Rubin, S., Rohatyn, S., Tatarinov, F., Rotenberg, E., Ramati, E., Dicken, U.,
751 Preisler, Y., Fredj, E., Yakir, D., and Tas, E.: Investigation of ozone deposition to vegetation under warm and
752 dry conditions near the Eastern Mediterranean coast, *Science of The Total Environment*, 658, 1316–1333,
753 doi:10.1016/j.scitotenv.2018.12.272, 2019.
- 754 Li, Q., Lerner, G., Bar, E., Lewinsohn, E., and Tas, E.: Impact of meteorological conditions on BVOC emission
755 rate from Eastern Mediterranean vegetation under drought, *EGUsphere* [preprint],
756 <https://doi.org/10.5194/egusphere-2024-529>, 2024.
- 757 Li, R., Warneke, C., Graus, M., Field, R., Geiger, F., Veres, P. R., Soltis, J., Li, S.-M., Murphy, S. M., Sweeney, C.,
758 Pétron, G., Roberts, J. M., and Gouw, J. de: Measurements of hydrogen sulfide (H₂S) using PTR-MS:
759 Calibration, humidity dependence, inter-comparison and results from field studies in an oil and gas
760 production region, *Atmos. Meas. Tech.*, 7, 3597–3610, doi:10.5194/amt-7-3597-2014, 2014.
- 761 Llusia, J., Roahytyn, S., Yakir, D., Rotenberg, E., Seco, R., Guenther, A., and Peñuelas, J.: Photosynthesis, stomatal
762 conductance and terpene emission response to water availability in dry and mesic Mediterranean forests,
763 *Trees*, 30, 749–759, doi:10.1007/s00468-015-1317-x, 2016.
- 764 Loewenstein, N. J. and Pallardy, S. G.: Drought tolerance, xylem sap abscisic acid and stomatal conductance
765 during soil drying: A comparison of canopy trees of three temperate deciduous angiosperms, *Tree
766 Physiology*, 18, 431–439, doi:10.1093/treephys/18.7.431, 1998.
- 767 Loreto, F. and Schnitzler, J.-P.: Abiotic stresses and induced BVOCs, *Trends in plant science*, 15, 154–166,
768 doi:10.1016/j.tplants.2009.12.006, 2010.
- 769 Maseyk, K. S., Lin, T., Rotenberg, E., Grünzweig, J. M., Schwartz, A., and Yakir, D.: Physiology-phenology
770 interactions in a productive semi-arid pine forest, *New Phytol*, 178, 603–616, doi:10.1111/j.1469-
771 8137.2008.02391.x, 2008.
- 772 Monson, R. K., Jaeger, C. H., Adams, W. W., Driggers, E. M., Silver, G. M., and Fall, R.: Relationships among
773 Isoprene Emission Rate, Photosynthesis, and Isoprene Synthase Activity as Influenced by Temperature,
774 *PLANT PHYSIOLOGY*, 98, 1175–1180, 1992.
- 775 Moradi, P., Ford-Lloyd, B., and Pritchard, J.: Metabolomic approach reveals the biochemical mechanisms
776 underlying drought stress tolerance in thyme, *Analytical biochemistry*, 527, 49–62,
777 doi:10.1016/j.ab.2017.02.006, 2017.
- 778 Murphy, B. L. and Morrison, R. D.: *Introduction to environmental forensics*, 2014.
- 779 Naor, R., Potchter, O., Shafir, H., and Alpert, P.: An observational study of the summer Mediterranean Sea
780 breeze front penetration into the complex topography of the Jordan Rift Valley, *Theor Appl Climatol*, 127,
781 275–284, doi:10.1007/s00704-015-1635-3, 2017.



- 782 Niinemets, U.: Mild versus severe stress and BVOCs: Thresholds, priming and consequences, *Trends in plant*
783 *science*, 15, 145–153, doi:10.1016/j.tplants.2009.11.008, 2010.
- 784 Niinemets, U., Loreto, F., and Reichstein, M.: Physiological and physicochemical controls on foliar volatile
785 organic compound emissions, *Trends in plant science*, 9, 180–186, doi:10.1016/j.tplants.2004.02.006,
786 2004.
- 787 Niinemets, Ü. and Monson, R. K. (Eds.): *Biology, Controls and Models of Tree Volatile Organic Compound*
788 *Emissions*, Springer Netherlands, Dordrecht, 2013.
- 789 Niinemets, Ü. and Reichstein, M.: Controls on the emission of plant volatiles through stomata: A sensitivity
790 analysis, *J. Geophys. Res.*, 108, 547, doi:10.1029/2002jd002626, 2003.
- 791 Nobel, P. S.: *Physicochemical & environmental plant physiology*, 2nd ed., Academic Press, San Diego, xxiv, 474,
792 1999.
- 793 Nobel, P. S.: *Physicochemical and Environmental Plant Physiology*, Elsevier Science, San Diego, CA, USA, 1
794 ressource en ligne (604, 2009).
- 795 Ormeño, E., Fernandez, C., Bousquet-Mélou, A., Greff, S., Morin, E., Robles, C., Vila, B., and Bonin, G.:
796 Monoterpene and sesquiterpene emissions of three Mediterranean species through calcareous and
797 siliceous soils in natural conditions, *Atmospheric Environment*, 41, 629–639,
798 doi:10.1016/j.atmosenv.2006.08.027, 2007.
- 799 Park, J.-H., Goldstein, A. H., Timkovsky, J., Fares, S., Weber, R., Karlik, J., and Holzinger, R.: Active atmosphere-
800 ecosystem exchange of the vast majority of detected volatile organic compounds, *Science (New York, N.Y.)*,
801 341, 643–647, doi:10.1126/science.1240961, 2013.
- 802 Pegoraro, E., Rey, A., Barron-Gafford, G., Monson, R., Malhi, Y., and Murthy, R.: The interacting effects of
803 elevated atmospheric CO₂ concentration, drought and leaf-to-air vapour pressure deficit on ecosystem
804 isoprene fluxes, *Oecologia*, 146, 120–129, doi:10.1007/s00442-005-0166-5, 2005.
- 805 Pegoraro, E., Rey, A., Greenberg, J., Harley, P., Grace, J., Malhi, Y., and Guenther, A.: Effect of drought on
806 isoprene emission rates from leaves of *Quercus virginiana* Mill, *Atmospheric Environment*, 38, 6149–6156,
807 doi:10.1016/j.atmosenv.2004.07.028, 2004.
- 808 Peñuelas, J. and Munné-Bosch, S.: Isoprenoids: An evolutionary pool for photoprotection, *Trends in plant*
809 *science*, 10, 166–169, doi:10.1016/j.tplants.2005.02.005, 2005.
- 810 Peñuelas, J., Rutishauser, T., and Filella, I.: Ecology. Phenology feedbacks on climate change, *Science (New*
811 *York, N.Y.)*, 324, 887–888, doi:10.1126/science.1173004, 2009.
- 812 Peñuelas, J. and Staudt, M.: BVOCs and global change, *Trends in plant science*, 15, 133–144,
813 doi:10.1016/j.tplants.2009.12.005, 2010.
- 814 Potosnak, M. J., LeSturgeon, L., Pallardy, S. G., Hosman, K. P., Gu, L., Karl, T., Geron, C., and Guenther, A. B.:
815 Observed and modeled ecosystem isoprene fluxes from an oak-dominated temperate forest and the
816 influence of drought stress, *Atmospheric Environment*, 48, 314–322, doi:10.1016/j.atmosenv.2013.11.055,
817 2014.
- 818 Ravikovitch, R., Koyumdjisky, H., Dan, Y., and others: Soils of Western and central valley of Yizreel, *Agric. Res.*
819 *Stn. Israel Bull.*, 64, 1960.
- 820 Reichstein, M., Falge, E., Baldocchi, D., Papale, D., Aubinet, M., Berbigier, P., Bernhofer, C., Buchmann, N.,
821 Gilmanov, T., Granier, A., Grunwald, T., Havrankova, K., Ilvesniemi, H., Janous, D., Knohl, A., Laurila, T.,
822 Lohila, A., Loustau, D., Matteucci, G., Meyers, T., Miglietta, F., Ourcival, J.-M., Pumpanen, J., Rambal, S.,
823 Rotenberg, E., Sanz, M., Tenhunen, J., Seufert, G., Vaccari, F., Vesala, T., Yakir, D., and Valentini, R.: On the



824 separation of net ecosystem exchange into assimilation and ecosystem respiration: Review and improved
825 algorithm, *Global Change Biol*, 11, 1424–1439, doi:10.1111/j.1365-2486.2005.001002.x, 2005.

826 Rohatyn, S., Rotenberg, E., Ramati, E., Tatarinov, F., Tas, E., and Yakir, D.: Differential Impacts of Land Use and
827 Precipitation on 'Ecosystem Water Yield', *Water Resour. Res.*, doi:10.1029/2017WR022267, 2018.

828 Sander, R.: Compilation of Henry's law constants (version 5.0.0) for water as solvent, *Atmos. Chem. Phys.*, 23,
829 10901–12440, doi:10.5194/acp-23-10901-2023, 2023.

830 Schade, G. W., Goldstein, A. H., and Lamanna, M. S.: Are monoterpene emissions influenced by humidity?,
831 *Geophys. Res. Lett.*, 26, 2187–2190, 1999.

832 Seco, R., Karl, T., Turnipseed, A., Greenberg, J., Guenther, A., Llusia, J., Peñuelas, J., Dicken, U., Rotenberg, E.,
833 Kim, S., and Yakir, D.: Springtime ecosystem-scale monoterpene fluxes from Mediterranean pine forests
834 across a precipitation gradient, *Agricultural and Forest Meteorology*, 237–238, 150–159,
835 doi:10.1016/j.agrformet.2017.02.007, 2017.

836 Sharkey, T. D. and Loreto, F.: Water stress, temperature, and light effects on the capacity for isoprene emission
837 and photosynthesis of kudzu leaves, *Oecologia*, 95, 328–333, doi:10.1007/Bf00320984, 1993.

838 Staudt, M., Wolf, A., and Kesselmeier, J.: Influence of environmental factors on the emissions of gaseous
839 formic and acetic acids from orange (*Citrus sinensis* L.) foliage, *Biogeochemistry*, 48, 199–216,
840 doi:10.1023/A:1006289120280, 2000.

841 Tiiva, P., Faubert, P., Rätty, S., Holopainen, J. K., Holopainen, T., and Rinnan, R.: Contribution of vegetation and
842 water table on isoprene emission from boreal peatland microcosms, *Atmospheric Environment*, 43, 5469–
843 5475, doi:10.1016/j.atmosenv.2009.07.026, 2009.

844 Tingey, D., Turner, D., and Weber, J.: Factors Controlling the Emissions of Monoterpenes and Other Volatile
845 Organic Compounds, U.S. Environmental Protection Agency, Washington, D.C., EPA/600/D-90/195 (NTIS
846 PB91136622), 1990.

847 Trowbridge, A. M. and Stoy, P. C.: BVOC-Mediated Plant-Herbivore Interactions, in: *Biology, Controls and*
848 *Models of Tree Volatile Organic Compound Emissions*, Niinemets, Ü., and Monson, R. K. (Eds.), Springer
849 Netherlands, Dordrecht, 21–46, 2013.

850 Wang, H., Lu, X., Seco, R., Stavrakou, T., Karl, T., Jiang, X., Gu, L., and Guenther, A. B.: Modeling Isoprene
851 Emission Response to Drought and Heatwaves Within MEGAN Using Evapotranspiration Data and by
852 Coupling With the Community Land Model, *Journal of advances in modeling earth systems*, 14,
853 e2022MS003174, doi:10.1029/2022MS003174, 2022.

854 Wold, S., Esbensen, K., and Geladi, P.: Principal component analysis, *Chemometrics and Intelligent Laboratory*
855 *Systems*, 2, 37–52, doi:10.1016/0169-7439(87)80084-9, 1987.

856 Zheng, Y., Unger, N., Tadić, J. M., Seco, R., Guenther, A. B., Barkley, M. P., Potosnak, M. J., Murray, L. T.,
857 Michalak, A. M., Qiu, X., Kim, S., Karl, T., Gu, L., and Pallardy, S. G.: Drought impacts on photosynthesis,
858 isoprene emission and atmospheric formaldehyde in a mid-latitude forest, *Atmospheric Environment*, 167,
859 190–201, doi:10.1016/j.atmosenv.2017.08.017, 2017.

860